www.amlett.com, www.vbripress.com/aml, DOI: 10.5185/amlett.2015.5868 Published online by the VBRI press in 2015

Surface and thermoluminescence study of Dy^{3+} doped $Sr_3B_2O_6$ nanocrystalline phosphor

Neharika[1], Vinay Kumar[1,2*], Jitendra Sharma[1] ,O.M. Ntwaeaborwa[2] , H.C. Swart[2]

[1]*School of Physics, Shri Mata Vaishno Devi University, Katra 182320 (J&K), India*
[2]*Department of Physics, University of the Free State, P.O. Box 339, Bloemfontein 9300, South Africa*

[*]Corresponding author. Tel: (+91) 1991285699 Ext. 2509; E-mail: vinaykdhiman@yahoo.com; vinaykumar@smvdu.ac.in

Received: 23 February 2015, Revised: 20 March 2015 and Accepted: 21 March 2015

ABSTRACT

In this letter, the thermoluminescence response and surface properties of $Sr_3B_2O_6:Dy^{3+}$ nanophosphor prepared by combustion method exposed to γ–rays are reported. The crystalline structure of nanophosphors was confirmed by X-ray powder diffraction. The result indicates rhombohedral nanocrystalline structure with an average grain size of 41 nm. The microstructure and morphology were studied by transmission electron microscopy, which show nanowire like structure with an average diameter of 42 nm. The samples were irradiated with a γ-dose using ^{60}Co source in the range of 100 Gy – 5000 Gy. The kinetic parameter such as activation energy (E), order of kinetics (b), and frequency factor (s) of the main glow peaks of the $Sr_3B_2O_6:Dy^{3+}$ sample at 5000 Gy and different heating rates were determined using both the TLAnal program and Chen's method. The effect of different heating rate at a fixed dose is discussed. X-ray photoelectron spectroscopy was used to study the surface chemical composition and the electronic states. Copyright © 2015 VBRI Press.

Keywords: Nanocrystalline phosphors; XPS; thermoluminescence.

Neharika obtained M. Sc. in Physics from SMVD University, Katra India in 2012. She is presently doing Ph.D at Shri Mata Vaishno Devi University, Katra (J&K). She is currently working in the area of development of phosphors for their potential application in solid state lighting, LED'S, radiation dosimetry etc.

Vinay Kumar received his Ph.D. from K.U.,Kurukshetra in 2007. His research interests are in fluorescent nanomaterials in powder and their applications in lighting, displays, and latent finger-print development. He has published more than 52 international peer reviewed research articles. Currently, Dr. Kumar is an Assistant Professor of Physics at the Shri Mata Vaishno Devi University, India. He is also a Life member of Luminescence Society of India.

Jitendra Sharma is Director, School of Physics at Shri Mata Vaishno Devi (SMVD) University, Katra. He received his Ph.D. in Physics from Jawaharlal Nehru University, New Delhi in the year 2001. He did his postdoctoral research at the Department of Chemistry, University of Durham, England (UK) and IRC (Inter-disciplinary Research Centre) for Polymer Chemistry. He was a senior postdoctoral fellow at the Department of Chemical and Biomolecular Engineering, University of Houston, Houston, Texas (USA) from 2006 to 2008.

Introduction

Thermoluminescence (TL) is a well known phenomenon and is used in diverse fields such as dosimetry, archaeology, geology, biology, biochemistry, forensic science, space science, thermo stimulated luminescence (TSL) photography, and radiation physics **[1]**. When an insulator or semiconductor is exposed to ionizing radiation, mobile electrons and holes are produced, and some of them are trapped at structural defects or impurity sites called traps. The trapped electrons can be released if sufficient energy is applied to the crystal, and when such electrons re-combine with a trapped hole, light is emitted which is produced by a release of the radiation induced electrons from the traps of the materials. TL is observed under three conditions. Firstly, the phosphors must be either a semiconductor or an insulator. Secondly, the material must have an ability to store energy when exposed to ionizing radiations. Thirdly, the luminescence emission is released by heating the material.

In the borates family, TSL glow curves and TSL emission characteristics were studied by many authors using the TL technique for radiation dosimetry **[2-5]**. The advantage of this kind of material is that it has a very low cost and easy to handle. Recently, boron compounds, both natural and synthesized have attracted attention in high technology utilization areas owing to their special crystal and optical characteristics. Lithium borates like lithium tetraborate ($Li_2B_4O_7$) and lithium triborate (LiB_3O_5) have

attractive features due to their interesting chemical structure. Also, lithium tetraborate has interesting optical properties **[6-7]**. Borates possess large electronic band gaps, attractive nonlinear optical (NLO) properties, chemical and environmental stability, and mechanical strength. Borates have strong absorption in vacuum ultra violet and this makes them strong phosphors, which give bright emission **[8]**. Borates are appropriate for the use in plasma displays and in laser technology due to high ultra violet (UV) transmittance at wavelengths down to 155 nm.[8] Recently many researchers have developed new mixed alkaline earth metal borates **[9]**. These are having good TL properties. Borates like $CsLiB_6O_{10}$ and $K_2Al_2B_2O_7$ discovered recently are reported to have potential application in NLO generating UV and vacuum UV laser radiation **[10]**. Alkaline-earth borates provide a new class of a potential host with a large band gap and covalent bond energy. TL studies on the alkaline earth borate like SrB_4O_7:Dy^{3+} has already been reported **[11]**.

In this paper, we present the surface investigations on the nanocrystalline Dy^{3+} doped nanophosphor prepared by combustion synthesis. Our main aim is to study the TL mechanism occurring in $Sr_3B_2O_6$:Dy^{3+} nanophosphor and to get knowledge about trapping parameters such as order of kinetics, activation energy and the frequency factor. These trap parameters describe the trap emitting centers responsible for the TL emission associated with TL glow peaks. Also, lack of knowledge about the trap parameters in the Dy^{3+} doped $Sr_3B_2O_6$ led us to do the TL study on $Sr_3B_2O_6$:Dy^{3+} crystalline phosphors exposed to γ-rays from a 60Co source. Effect of different heating rates on the glow curves has been discussed. The TLAnal program was used to analyze the TL glow curves **[12]**. TL kinetic parameter studies were carried out to explore trapping dynamics and an effort was made to effectively compute trapping parameters for the $Sr_3B_2O_6$:Dy^{3+}.

Experimental

Combustion method was used to synthesize $Sr_3B_2O_6$:Dy^{3+} phosphors at 600^0 C using raw materials $Sr(NO_3)_3$, H_3BO_3, NH_2CONH_2, Dy_2O_3 and HNO_3. The appropriate amount of reactants were dissolved in distilled water and were thoroughly mixed using a mortar and pestle to obtain a homogeneous mixture and placed in a preheated muffle furnace at 600℃. It was milled gently and then annealed at 900℃ for 3 hours to improve crystalinity. The structural characterization of the samples was carried out by X-ray diffraction (XRD) using a Bruker Advance D8 X-ray diffractometer with Cu Kα radiation source (=0.15406nm). The particle morphology was studied by Hitachi transmission electron microscope. X-ray photoelectron spectroscopy (XPS) analysis were carried out using a PHI5000 Versaprobe spectrometer (analyser resolution ≤0.5 eV) using monochromatic Al Kα radiation ($h\nu$ = 1253.6 eV). For TL spectroscopy, the samples were pre-exposed to γ-radiation at room temperature by using a gamma chamber containing a ^{60}Co source at the Health Physics Laboratory at Inter University Accelerator Centre, New Delhi. The TL glow curves of the exposed phosphors were recorded by taking 5 mg of the sample each time on the HARSHAW QS 3500 TLD reader, at different heating rate $3K/s$, $5K/s$ and $10K/s$.

Results and discussion

X-Ray diffraction study

The pattern exhibits a pure phase of Sr3B2O6 which matches well with JCPDS card No-31-1343 as shown in **Fig. 1**. $Sr_3B_2O_6$:Dy^{3+} samples show a rhombohedral structure with a space group of R-3c and lattice constants a = 9.0552 Å, b= 9.0552 Å, c = 1.2566 Å, cell volume = 8.9603 $Å^3$ after annealing and were calculated using POWD program **[13]**.

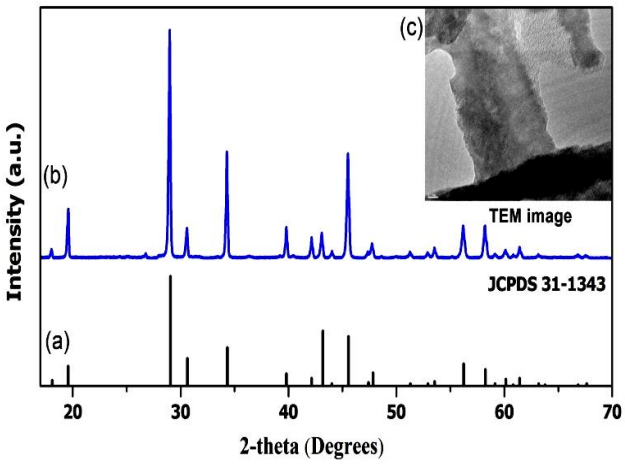

Fig. 1. XRD patterns of **(a)** JCPDS 31-1343 **(b)** $Sr_3B_2O_6$:Dy^{3+} and **(c)** TEM image of $Sr_3B_2O_6$:Dy^{3+} nanowire (inset).

The average particle size was calculated as 41nm by using Scherrer's equation from the most intense peaks.

$$d = \frac{0.89\lambda}{\beta \cos \theta_B} \quad (1)$$

Where d the average diameter of the nanoparticles is, λ is the wavelength of Cu K_α(1.54Å) radiation, β (in radians) is the full width half maxima (FWHM) and θ_B is the Bragg angle **[14-15]**.

TEM study

The morphology of the $Sr_3B_2O_6$:Dy^{3+} phosphor is shown in the inset of **Fig. 1**. The diameter (d) of the nanowires was found to be 42 nm. The length of the $Sr_3B_2O_6$:Dy^{3+} nanowires was found to differ considerably. The average particle size obtained from XRD (~41nm) for $Sr_3B_2O_6$:Dy^{3+} nanowires are almost the same when compared to the diameter (~42 nm) obtained from the TEM studies.

XPS study

XPS is a surface-sensitive quantitative spectroscopic technique which is used to examine elemental composition and oxidation states of the cations. **Fig. 2(a)** shows the survey scan XPS spectrum of $Sr_3B_2O_6$:Dy^{3+} nanophosphor and confirms the presence of Sr, B, O and Dy from their corresponding binding energies.

Fig. 2(b) shows high resolution scan for Sr 3d core level. Two doublets appear in the Sr 3d spectra, one was attributed to oxygen coordinated Sr in the $Sr_3B_2O_6$ lattice for which $3d_{5/2}$ and $3d_{3/2}$ spin order split components are

located at B.E.'s of 133.2 eV and 135.1 eV respectively **[16]**. Sr-O chemical bonds are commonly classified as very ionic with complete transfer of valence e-s from Sr to O atomsas reported by Atuchin **[17]**. B.E of Sr 3 the $d_{5/2}$ line is not expected to change much in different Sr- bearing oxides. The other component resembles the metallic Sr bonding at B.E.'s of 134.3 eV and 136.1 eV for Sr $3d_{5/2}$ and $3d_{3/2}$, respectively. This signal could arise from the Sr residing at the surface terminated Sr sites (metallic nature) at interstitial positions in $Sr_3B_2O_6$.

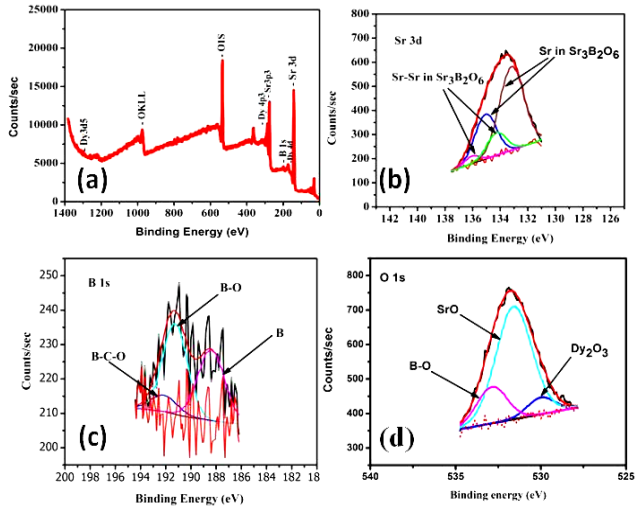

Fig. 2. (a) XPS survey scan spectrum of the $Sr_3B_2O_6$:Dy^{3+} nanophosphors and XPS high-resolution scan with the deconvolution for **(b)** Sr 3d core level **(c)** B 1s core level and **(d)** O 1s core level.

Fig. 2(c) shows the B 1s core level photoelectron spectra in the $Sr_3B_2O_6$ lattice. The asymmetrical nature of the peak suggests that a distribution of B chemical states exists. The XPS spectrum of boron was deconvoluted into three peaks. The binding energy of one of the component at 192.2 eV can be assigned to the B-C-O bonding. The presence of C atoms is attributed to adventitious C from hydrocarbons, C-O-C, C-OH, species during combustion synthesis of $Sr_3B_2O_6$. The peak at a B.E. around 191.3 eV can be assigned to photoelectrons originating from B atoms bonded to oxygen atoms (B-O) in the host lattice. Also, the peak at the lower B.E. of 188.5 eV corresponds to B metallic bond in $Sr_3B_2O_6$ lattice **[18]**.

Fig. 2(d) shows the O 1s core level photoelectron spectra in the $Sr_3B_2O_6$ lattice. The XPS spectrum of O1s core level scan in the host matrix was deconvoluted into three components representing different lattice sites of oxygen in the $Sr_3B_2O_6$ nanophosphor. The component corresponding to binding energy of 191.3 eV was due to oxidation of boron. This B-O bond result in the presence of an O1s feature at higher binding energy of 532.9 eV as in **Fig. 2(c)**. The second component in O1s core level with a binding energy of 531.6 eV corresponds to oxygen coordinated Sr bond in $Sr_3B_2O_6$ lattice for which $3d_{5/2}$ and $3d_{3/2}$ spin order split components were located at B.E.'s of 133.2 eV and 135.1 eV respectively in **Fig.2. (b)** The third component at a binding energy of 530.00 eV corresponds to Dy_2O_3 bond in O1s core level for $Sr_3B_2O_6$ lattice **[19]**.

Thermoluminescence study

The effect of different doses of γ-radiation (100Gy - 5000Gy) on the TL glow curve of $Sr_3B_2O_6$:Dy^{3+} nanophosphor was investigated. The recorded TL glow curves show a broad TL peak which is mainly due to superposition of a distribution of second order TL peaks **(Fig. 3)**. Dose response curve of $Sr_3B_2O_6$:Dy^{3+} nanocrystalline phosphor is also shown in the inset of **Fig. 3**.

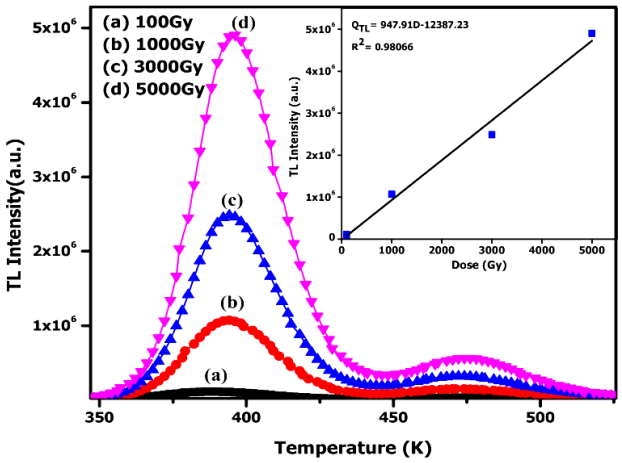

Fig. 3. TL Glow curve of $Sr_3B_2O_6$:Dy^{3+} nanocrystalline phosphor after different γ - radiation doses with its dose response curve (shownin inset).

A change in TL glow curves at low doses and high doses was observed with a significant peak shift from 388 K to 396 K. Peak shiftedslightly towards higher temperature with dose. This indicates that the TL glow peak obeyed a non-first order kinetics, which could be attributed to the creation of deep level traps [15, 20]. With the increase in dose, luminescent center increases which leads to an increase in peak intensity. The higher the exposure to ionizing radiation, the higher number of electrons and holes are trapped hence the TL intensity peak increase with an increasing γ -ray dose. Also, a linear response having R^2 = 0.98066 is observed which is possible only when yield or efficiency (Y_{TL}) of thermoluminescent emission is constant, as the TL signal from the phosphor (Q_{TL}) is proportional to dose (D) and yield or efficiency (Y_{TL}) of thermoluminescent emission **[21]**. Effect of different heating rates on the TL response of the $Sr_3B_2O_6$:Dy^{3+} nanocrystalline phosphor is shown in **Fig. 4**. It can be seen that the glow peak height increased with the increase in the heating rate and the peak position shifted toward a higher temperature, Which shows that the charge carriers (electrons or holes) travelling towards the recombination centers for producing the desired luminescence have enough time to get retrapped **[22-23]**.

Kinetic parameters

Computerized glow curve deconvolution is widely used for studying the TL mechanism as well as for TL dosimetry **[24-25]**. We have used the TL glow curve analyzer program version 1.0.3. This program is used to deconvolute TL glow curves and to compute trapping parameters such asactivation energy (E_α) and frequency factor (s). **Fig. 5** shows, deconvoluted peaks of $Sr_3B_2O_6$:Dy^{3+} nanocrystalline phosphor at 5000 Gy at 10K/s analyzed by the graphical

user interface of the TLAnal program. We have reported the trapping parameters obtained after deconvolution of the TL glow peaks of the $Sr_3B_2O_6$:Dy^{3+} nanocrystalline phosphor at different heating rates by the TLAnal program in **Table 1**.

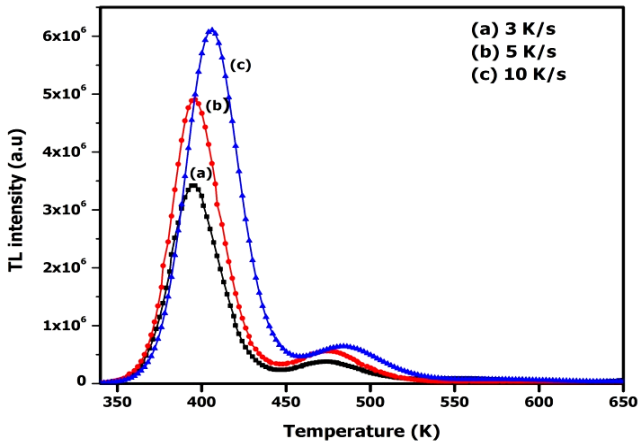

Fig. 4. TL glow curve for $Sr_3B_2O_6$: Dy^{3+} nanocrystalline phosphor at 5000 Gy at 3K/s, 5K/s and 10K/s.

Table 1. Kinetic parameters of the deconvoluted peaks of $Sr_3B_2O_6$: Dy^{3+} at 5000 Gy at different heating rate by TLAnal program and Chen's method.

$Sr_3B_2O_6$: Dy^{3+}	Peak	T_m (K)	Order of Kinetics b (μ_g)	Activation energy E (eV)		Frequency factor S (s^{-1})	
				TLAnal program	Chen's formula	TLAnal program	Chen's formula
Heating rate 3 K s^{-1}	1	392	2 (0.50)	1.54	1.52	4.22×10^{19}	1.60×10^{19}
	2	405	2 (0.53)	1.53	1.53	0.58×10^{19}	1.66×10^{19}
	3	474	2 (0.52)	1.30	1.28	2.25×10^{13}	0.98×10^{13}
Heating rate 5 K s^{-1}	1	390	2 (0.47)	1.56	1.56	0.79×10^{20}	1.00×10^{20}
	2	402	2 (0.51)	1.45	1.40	6.96×10^{17}	1.98×10^{17}
	3	474	2 (0.54)	1.46	1.46	1.27×10^{15}	1.44×10^{15}
Heating rate 10 K s^{-1}	1	408	2 (0.51)	1.42	1.41	4.07×10^{17}	2.58×10^{17}
	2	394	1 (0.40)	1.40	1.35	1.12×10^{18}	0.05×10^{18}
	3	484	2 (0.54)	1.36	1.36	1.00×10^{14}	1.05×10^{14}

The kinetic parameters E, b and s of each of the deconvoluted glow peaks of the TL materials were also calculated by Chen's set of empirical formulae for the Glow curve method, **Table 1 [26-27]**. Peak Temperature T_m, the low and high temperature half heights at T_1 and T_2 were utilized. Theoretically, the the value of the geometrical factor, (μ_g), gives the order of kinetics, which can be evaluated from equation (1). The values of μ_g for first order kinetics must be close to 0.42 and for second order kinetics μ_g value must be close to 0.52. The deconvolution of the glow curves was done by using the TLAnal Program given by Chen *et al* **[12]**.

$$\mu_g = \frac{T_2 - T_m}{T2 - T1} \qquad (2)$$

The activation energy (E_α) can be calculated from the thermal peak temperature by using the following equation:

$$E_\alpha = c_\alpha \left(\frac{kT_m^2}{\alpha}\right) - b_\alpha (2kT_m) \qquad (3)$$

With

$$\alpha = \tau, \delta, \omega; \quad \tau = T_m - T_1; \delta = T_2 - T_m; \omega = T2 - T1;$$
$$c_\tau = 1.51 + 3.0\left(\mu_g - 0.42\right); \; c_\delta = 0.976 + 7.3\left(\mu_g - 0.42\right); c_\omega = 2.52 + 10.2\left(\mu_g - 0.42\right); b_\tau = 1.58 + 4.2\left(\mu_g - 0.42\right); b_\delta = 0; b_\omega = 1.$$

After calculating activation energy (E) and order of kinetic (b), the frequency factor was calculated from the following equation (3)

$$\frac{\beta E}{kT_m^2} = s \exp\left\{\frac{-E}{kT_m}\right\}[1 + (Z-1)\Delta_m] \qquad (4)$$

E = Activation energy (eV) and $\Delta = 2kT/E$.

The parameters calculated from both the TLAnal program and Chen's method was found to be in good agreement with each other. Mostly the second order kinetics was observed and the trap levels varied between 1.28 and 1.56 eV having frequency factor ranging from 0.98×10^{13} to 0.79×10^{20} s^{-1}.

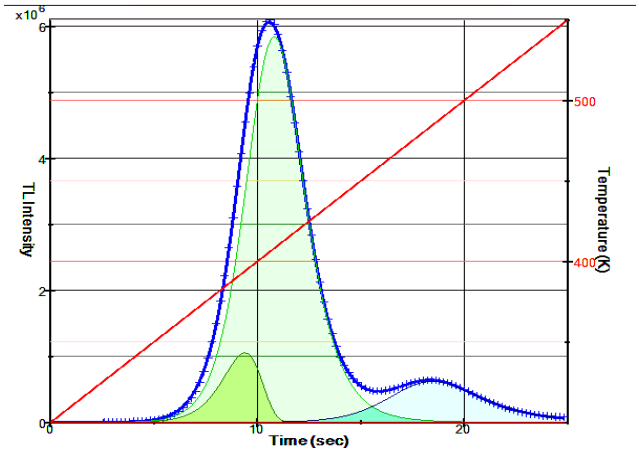

Fig. 5. The deconvoluted peaks of $Sr_3B_2O_6$:Dy^{3+} nanocrystalline phosphor at 5000 Gy at 10K/s analyzed by graphical user interface of TLAnal program. Figure of merit (FOM) of about 0.709% is also shown.

Conclusion

The long afterglow phosphors with Dy^{3+} doped in the $Sr_3B_2O_6$ were synthesized successfully using combustion method. The morphology was studied by transmission electron microscopy which showed a nanowire like structure. The XPS study confirms the presence of Sr, B, O and Dy on the surface of the phosphor. The synthesized phosphors were irradiated with different γ-doses in the range of 100 to 5000 Gy. A shift was observed towards higher temperatures in the emission peak temperature as the dose increased, indicating a non-first order kinetics, which could be attributed to the creation of deep level defects, caused by the irradiation. The TL intensity was found to be linear with γ-dose. In addition, the TL parameters were also studied by using both TLAnal program and Chen's method. The activation energy and frequency factor obtained by both TLAnal program and Chen's method were found to be in good agreement with each other.

Acknowledgements
The authors are thankful to IUAC, New Delhi for providing facilities for gamma-radiation and recording TL. One of the author (Neharika) is also

greatly thankful to BRNS, Department of Atomic energy and Govt. of India for financial support under project 2012/34/37/BRNS/1035.

Reference

1. Zhang, Y.; Chen, X.L.; Liang, J.K.; Xuet, T.; *J. Alloys Compd.*, **2003** *348*, 314. **DOI:** 10.1016/S0925-8388(02)00843-5
2. Knitel, M.J.; Dorenbos, P.; van Eijk, C.W.E.; Plasteig, B.; Viana, B.; Kahn-Harari, A.; Vivien, D.; *Nucl. Instrum. Meth. Phys. Res. A* **2000** *443*, 364. **DOI:** 10.1016/S0168-9002(99)01154-7
3. Sangeeta; Sabharwal, S.C.; *J. Lumin.***2003** *104*, 267. **DOI:** 10.1016/S0022-2313(03)00080-2
4. Furetta, C.; Kitis, G.; Weng, P.S.; Chu. T.C.; *Nucl. Instrum. Meth. Phys. Res. A* **1999** *420*, 441. **DOI:** 10.1016/S0168-9002(98)01198-X
5. Prokic, M.; *Radiat. Meas.***2001** *33*, 393. **DOI:** 10.1016/S1350-4487(01)00039-7
6. Pekpak. E.; *Open Miner. process J* **2010** *3*, 14.
7. V.S. Gorelik, A. V. Vdovin, V. N. Moiseenkoet al., *J. Russ. Laser Res.* **2003,** *24*, 553.. **DOI:** 10.1023/B:JORR.0000004168.99752.0e
8. Becker. P.; *Adv. Mater*. **1998** *10*, 979. **DOI:** 10.1002/(SICI)1521-4095(199809)10:13<979::AID-ADMA979>3.0.CO;2-N
9. Ramasamy. V.; Anishiaa. S.R.; Joseb. M.T.; Ponnusamyc. V.; *Arch. Phy. Res.* **2011** *2*, 1.
10. Kumbhakar. P.; Kobayashi. T.; *Appl. Phys. B* **2004** *78*, 165. **DOI:** 10.1007/s00340-003-1364-7
11. Li. J.; Hao. J.Q.; Li. C.Y.; Zhang. C.X.; Tang. Q.; Zhang. Y.L.; Su. Q.; Wang. S.b.; *Radiat. Meas.* **2005** *39*, 229. **DOI:** 10.1016/j.radmeas.2004.06.006
12. Chen, R.; Kirsh, Y. (1st edn.); Analysis of Thermally Stimulated Processes; Pergamon Press: New York, **1981**.
13. Wu, E.; POWD-An Interactive Powder Diffraction Data Interpretation and Indexing Program, Version 2.2 (School of Physical Sciences, Flinders Univ.,South Australia).
14. Cullity, B.D. (2nd edn); Elements of X-ray Diffraction; Addison-wesley press: New York, **1956**. **DOI:** elementsofxraydi030864mbp
15. Bedyal, A.K.; Kumar, V.; Lochab, S.P.; Singh, F.; Ntwaeaborwa, O.M.; Swart, H.C.; Int. *J. Mod. Phys.* **2013** *22*,365. **DOI:** 10.1142/S2010194513010386
16. Moulder, J.F.; Strikle, W.F.; Sobol P.E.; Bomben, K.D.; Handbook of X-ray photoelectron spectroscopy; Perkin- Elmer press: Minnesota, **1995**.
17. Atuchin, V.V.; Grivel, J.-C.; Korotkov, A.S.; Zhang Z.; *J. Solid State Chem.* **2008**, *181*, 1285. **DOI:** 10.1016/j.jssc.2008.01.046
18. Chenet, L.; Goto, T.; Hirai, T.; *J. Mater. Sci. Lett.* **1990**, *9*, 997. **DOI:** 10.1007/BF00727857
19. Sharma, D.D.; Rao, C.N.R.; *J. Electron. Spectrosc. Relat. Phenom.* **1980**, *20*, 25. **DOI:** 10.1016/0368-2048(80)85003-1
20. Furreta, C.; Handbook of Thermoluminescence; World scientific press: Italy, **1937**.
21. Fasasi, A.Y.; Balogun, F.A.; Fasasi, M.K.; Ogunleye, P.O.; Mokobia, C.E.; Inyang, E.P.; *Sens. Actuator A-Phys.* **2007**, *135*, 598. **DOI:** 10.1016/j.sna.2006.07.029
22. Bahl, S.; Pandey, A.; Lochab, S.P.; Aleynikov, V.E.; Molokanov, A.G.; Kumar., P.; *J. Lumin.* **2013**, *134*, 691. **DOI:** 10.1016/j.jlumin.2012.07.008
23. Kaur, N.; Singh, M.; Singh, L.; Lochab, S.P.; *Radiat. Phys. Chem.* **2013**, *87*, 26. **DOI:** 10.1016/j.radphyschem.2013.02.001
24. Chung, K.S.; Choe, H.S.; Lee, J.I.; Kim, J.L.; Chang, S.Y.; *Radiat. Prot. Dosim.* **2005**, *115*, 345. **DOI:** 10.1093/rpd/nci073
25. Chung, K.S.; Choe, H.S.; Lee, J.I.; Kim, J.L.; *Radiat. Meas.* **2007**, *42*, 731. **DOI:** 10.1016/j.radmeas.2007.02.028
26. Marwaha, G.L.; Singh, N.; Mathur, V.K.; *Mater. Res. Bull.* **1979**, *14*, 1489. **DOI:** 10.1016/0025-5408(72)90217-6
27. Kumar, V.; Kumar, R.; Lochab, S.P.; Singh, N.; *J. Phys. D: Appl. Phys.* **2006**, *39*, 5137. **DOI:** 10.1088/0022-3727/39/24/007
28. Bilski, P.; Obryk, B.; Olko, P.; Mandowska, E.; Mandowski, A.; Kim, J.L.; *Radiat. Meas.* **2008**, *43*, 315. **DOI:** 10.1016/j.radmeas.2007.10.015

